

Hydrogen Storage by Reduction of CO₂ to Synthetic Hydrocarbons

Kun Zhao, Wen Luo, Noris Gallandat, Jie Zhang, and Andreas Züttel*

Abstract: The storage of renewable energy is crucial for the substitution of fossil fuels with renewable energy. Hydrogen is the first step in the conversion of electricity from renewable sources to an energy carrier. However, hydrogen is technically and economically challenging to store, but can be converted with CO₂ from the atmosphere or oceans to hydrocarbons. The heterogeneously catalyzed gas phase reaction and the electrochemical CO₂ reduction are reviewed and the application of a new type of reactor is described. The mechanism of the gas phase CO₂ reduction on a heterogeneous catalyst is shown in detail and the function of the supported catalyst is explained. Finally, an economic estimation on the cost of synthetic methane is presented which leads to a cost of 0.3 CHF/kWh in CH₄.

Keywords: Electrochemical CO₂ reduction · Hydrogen · Methane synthesis · Renewable energy · Synthetic hydrocarbons



Kun Zhao graduated in 2012 with a B.S. in Applied Chemistry and B.S. in Physics from the Central China Normal University, Wuhan, China, followed by a M.S. in Physical Chemistry. From 2016 to 2020 she studied for a PhD in the group of Prof. Andreas Züttel, EPFL Valais, with the topic ‘Mechanisms of the Heterogeneously Catalyzed Reaction of CO₂ Hydrogenation on Transition Metal Surfaces’.

From 2021, she is working as a postdoc at the Department of Chemistry, University of Washington, Seattle, USA.



Wen Luo received his B.Sc. and M.Sc. degrees from Sichuan University, Chengdu, China, in 2009 and 2012, respectively. Then he joined Dr. Spiros Zafeiratos’ group, Université de Strasbourg, Strasbourg, France as a PhD candidate in physical chemistry, graduating in 2016. He is currently a postdoc in Prof. Andreas Züttel’s group in EPFL Valais. He is a SNF ambizione award winner in 2018 with the topic ‘Investigation of CO₂ hydrogenation on Metal Clusters with NAP-XPS’ (CO₂Clé).

hydrogenation on Metal Clusters with NAP-XPS’ (CO₂Clé).



Noris Gallandat graduated with a BSc in Mechanical Engineering from the ETH Zurich in 2012. He then went on to pursue graduate studies as a Fulbright Scholar at the Georgia Institute of Technology, USA, where he obtained MSc and PhD degrees in 2015. His doctoral thesis focused on the enhancement of ambient heat rejection in passive thermal management systems. In 2016, he joined the Laboratory of Materials

for Renewable Energy at EPFL Valais as a postdoctoral fellow. In Feb. 2017, he co-founded GRZ Technologies Ltd., a tech startup

aiming at commercializing hydrogen-related technologies. Since 2017 he is CEO of GRZ Technologies Ltd. and project leader of SOMAHR.



Jie Zhang was born in Zaoyang, China in 1989. In 2013 he graduated with a BS degree from Harbin Institute of Technology, China, followed by a MS in 2015. From 2015–2016 he worked as a quality engineer in TP-LINK Technologies Co., Ltd., China and from 2016 to 2017 as a research assistant in Southern University of Science and Technology, China. From 2018 he is a PhD student at EPFL, Valais in Sion, Switzerland.



Andreas Züttel was born 1963 in Bern, Switzerland. In 1985 he graduated with an engineering degree in Chemistry, from Burgdorf, Switzerland, followed by a Diploma in Physics from the University of Fribourg (UniFR), Switzerland in 1990. In 1993 he graduated as Dr. rer. nat. from the science faculty UniFR. In 1994 he worked as postdoc with AT&T Bell Labs in Murray Hill, New Jersey, USA. In 1997 he started as

lecturer at the Physics Department UniFR and in 2003 he was appointed an external professor at the Vrije Universiteit Amsterdam, Netherlands. In 2004 he completed his habilitation in experimental physics at the science faculty UniFR. President of the Swiss Hydrogen Association ‘HYDROPOLE’. He was appointed head of the section ‘Hydrogen & Energy’ at EMPA and Prof. tit. in the physics department UniFR in 2006. In 2009 he was a guest professor at IMR, Tohoku University in Sendai, Japan and in 2012 visiting professor at Delft Technical University, The Netherlands. 2014 Full Professor for Physical Chemistry, Institut des Sciences et Ingénierie Chimiques, EPFL, Switzerland. Since 2020 he is a member of the Swiss Academy of Technical Science.

*Correspondence: Prof. A. Züttel, E-mail: andreas.zuettel@epfl.ch

Laboratory of Materials for Renewable Energy (LMER), Institute of Chemical Sciences and Engineering (ISIC),

École Polytechnique Fédérale de Lausanne, EPFL Valais/Wallis, Switzerland and Empa Materials Science and Technology, Dübendorf, Switzerland

1. Hydrogen Storage in Hydrocarbons

Hydrogen is the first product in the transfer of renewable energy to a chemical energy carrier in the natural photosynthesis as well as in the technical processes (metal hydrides, Sabatier reaction, ammonia synthesis, *etc.*). Hydrogen as a renewable energy carrier has many advantages, *i.e.* the hydrogen cycle is a closed cycle realized by purely technical means (no living matter involved), the water as oxidation product precipitates on earth, and the power density is high: 1 kg H₂ is produced per 1 m² electrode surface in 1 h. However, due to its physical properties, hydrogen storage is a challenge, and the applications for hydrogen do not yet exist. On the other hand, the reduction of CO₂ to synthetic hydrocarbons leads to a product that is easy to store and all the applications already exist. However, CO₂ does not precipitate on earth and remains in the atmosphere at 400 ppm or dissolved in the ocean. The average concentration of inorganic carbon in the ocean is $\approx 2.3 \text{ mmol}\cdot\text{kg}^{-1}$ (40 ppm) and its residence time is $\approx 200^{\circ}000$ years. Approximately one quarter of the worldwide annually emitted CO₂ of 10 Gt dissolves in the ocean. The thermodynamic free energy for the concentration of 400 ppm CO₂ to 1 bar is $\Delta G = R\cdot T\cdot\ln(p/p_0)$ and is equal to 20 kJ/mole, which corresponds to 0.44 kWh/kg C. This is about 5% of the energy stored per kg of carbon.^[1] The main challenges are, therefore, the capture of the CO₂ from the atmosphere and the controlled reduction of the CO₂ with hydrogen to a specific product.

Two reactions are well established for the synthesis of hydrocarbons from CO₂: the Sabatier reaction: $\text{CO}_2 + 4\text{H}_2 \rightarrow \text{CH}_4 + 2\text{H}_2\text{O}$, and the reversed water gas shift reaction: $\text{CO}_2 + \text{H}_2 \rightarrow \text{CO} + \text{H}_2\text{O}$, combined with the Fischer-Tropsch reaction: $n\text{CO} + (2n+1)\text{H}_2 \rightarrow \text{CH}_3(-\text{CH}_2)_{n-2}-\text{CH}_3 + n\text{H}_2\text{O}$. The Sabatier reaction produces the most stable compound, *i.e.* methane. Methane activation, *i.e.* the linking of C atoms starting from methane is today only realized by the partial oxidation of methane ($\text{CH}_4 + 1.5\text{O}_2 \rightarrow \text{CO} + 2\text{H}_2\text{O}$, $\text{CH}_4 + \text{H}_2\text{O} \rightarrow \text{CO} + 3\text{H}_2$) followed by the Fischer-Tropsch synthesis. On the other side, the Fischer-Tropsch synthesis leads to a large variety of products, starting from methane to waxes and even leads to the deposition of carbon and tar on the catalysts.

The successful development of the new materials for the efficient absorption of CO₂ from the atmosphere, the production of hydrogen from renewable energy and the controlled reduction of CO₂ to the desired product, *e.g.* liquid hydrocarbons like diesel will allow fossil fuels to be replaced completely and introduce a closed cycle for energy materials.

The catalytic reduction of CO₂ depends on the local availability of hydrogen atoms, the binding and orientation of the CO₂ molecules on the surface of the catalyst and the bonding character between the C and O atoms and the surface atoms.^[2] Furthermore, the formation of C–C bonds could not be controlled until now and are randomly formed depending on the reaction conditions. The understanding of the Fischer-Tropsch process is that the conversion of CO to alkanes involves hydrogenation of CO, the dissociation of C–O bonds with H₂, and the formation of C–H and C–C bonds. The reactions are assumed to proceed on the surface of the catalyst *via* initial formation of surface-bound metal carbonyls. The CO ligand may undergo dissociation, possibly into oxide and carbide ligands.^[3] Other intermediates may be various C₁ fragments including formyl (CHO), hydroxycarbene (HCOH), hydroxymethyl (CH₂OH), methyl (CH₃), methylene (CH₂), methyldiyne (CH), and hydroxymethyldiyne (COH) as schematically shown in Fig. 1.

The distribution of the hydrocarbon products synthesized during the Fischer-Tropsch process^[4] is described as an Anderson-Schulz-Flory distribution,^[5] which is expressed as: $W_n/n = (1 - \alpha)^2 \alpha^{n-1}$ where W_n is the weight fraction of hydrocarbon molecules containing n carbon atoms, α is the probability for chain growth, *i.e.* the probability that a molecule will add an additional C to the chain. In general, the catalyst surface properties and the specific reaction conditions determine α to a large extent.

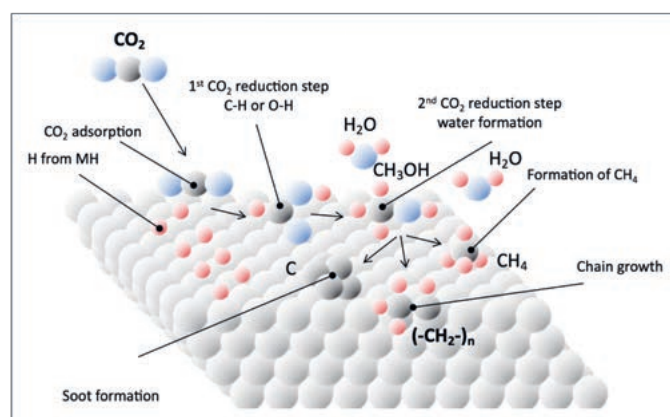


Fig. 1. Schematic model of the CO₂ reduction reaction pathways on the surface of a catalyst, *e.g.* metal, metal oxide or hydride.

Methane represents the largest single product according to the Anderson-Schulz-Flory equation for α less than 0.5. For α increasing approaching 1, the total amount of methane formed minimizes compared to the sum of all longer chain products ($n \geq 2$). The long-chained hydrocarbons ($n > 12$) are waxes, which are solid at room temperature. Therefore, for the production of liquid fuels for mobility it is necessary to crack the long-chained hydrocarbons of the Fischer-Tropsch products.

The detailed mechanism of the Fischer-Tropsch synthesis has been reviewed by Davis.^[6] Five schematics were discussed which differ mainly in the sequence of the C–H and O–H formation. Either CO chemisorbs on the metal site (M–C=O) and is reduced with hydrogen to M–CH–OH. These oxygenates react under condensation to form C–C bonds. Another possibility is that M–CH=O is formed, which is further reduced to M–CH₃ and then reacts with CO to form a C–C bond. Hydrogen may react solely with the oxygen in M–C=O and a carbide M₄C is formed which further reacts with hydrogen to M₂CH₂. The carbide can react with hydrogen and simultaneously form a C–C bond M–CH₂–CH₂–M. Finally, the M–CH₂ neighboring groups lead to the insertion of a second CH₂ on the same metal site CH₂–M–CH₂ and form a C–C bond.

The growth of the hydrocarbon chain can be sterically limited by using surface structuring, zeolites or other catalyst substrates with constrained size pores that restrict the formation of hydrocarbons longer than some characteristic size (usually $n < 10$). The reaction can be controlled so as to maximize the center of the distribution, *e.g.* around $n = 6$, *i.e.* to minimize methane formation without allowing the production of long-chained hydrocarbons. Such efforts have met with only limited success except for the methanol to gasoline process on ZSM-5 catalyst.^[7] Furthermore, and critical to the production of liquid fuels, are reactions that form C–C bonds, such as migratory insertion, the key process in the synthesis of carbon nanostructures like carbon nanotubes. Many related stoichiometric reactions have been simulated on discrete metal clusters, but homogeneous Fischer-Tropsch catalysts are poorly developed and not yet of commercial importance.^[8] Two new approaches are planned in order to control the reaction: First steric hindrance of the adsorbents by surface structuring as well as the use of nano-cavities. Second the change of the thermodynamic potential of the intermediates by the binding energy of the carbon atom to the substrate,^[9] *i.e.* tailoring the electronic structure of the surface. A first-principles theoretical study of carbon-carbon coupling in CO₂ electro reduction on the copper (211) surface was presented by Montoya *et al.*^[10] The kinetic barriers of the C–C bond formation between the adsorbents derived from CO were determined. The barriers decrease significantly with the progressing reduction, *i.e.* the degree of hydrogenation of the reacting adsorbents.

C₂₂ products from direct CO₂ hydrogenation are limited in the range of C₂–C₄ on a tandem or bifunctional catalyst.^[11–13] Ahead of investigating the C–C coupling, we explored the intrinsic interactions between the catalyst surface and the reactant gases. In this review, we present our recent research results on both the heterogeneously catalyzed CO₂ hydrogenation over gas/solid interface, and the electrochemical CO₂ reduction on the electrolyte/electrode interface. At the end, we also give an evaluation of the economics of the synthetic hydrocarbons.

2. Mechanism of CO₂ Reduction

2.1 Activation Energy and Equilibrium

In contrast to the CO₂ reduction in biosystems^[14] working at room temperature, the rather high activation energy of the CO₂ reduction with hydrogen requires high temperatures and/or highly active catalysts (Fig. 2). The enthalpy as well as the entropy for the reaction of hydrogen and carbon dioxide to hydrocarbons are negative, therefore, the thermodynamic limit for the yield of the reaction decreases with increasing temperature. Only the reduction of CO₂ to carbon monoxide is exothermic and has a positive entropy change.

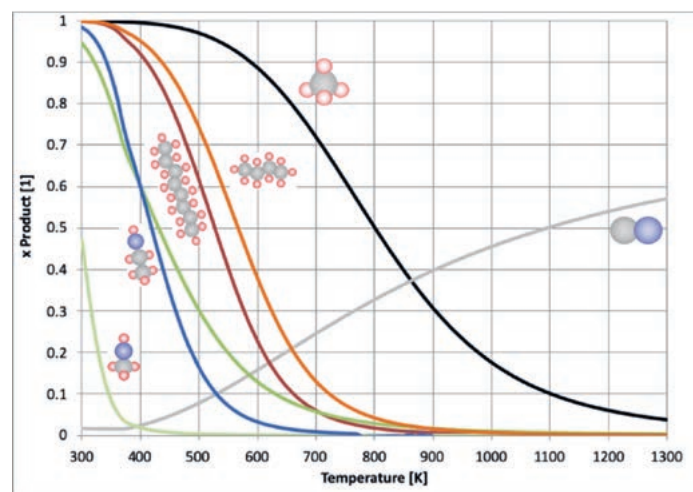


Fig. 2. Thermodynamic limit of the reaction for methane $\text{CO}_2 + 4\text{H}_2 \rightarrow \text{CH}_4 + 2\text{H}_2\text{O}$, hydrocarbons $n\text{CO}_2 + (3n+2)\text{H}_2 \rightarrow \text{C}_n\text{H}_{2n+2} + 2n\text{H}_2\text{O}$, methanol and ethanol $n\text{CO}_2 + (3n+1)\text{H}_2 \rightarrow \text{C}_n\text{H}_{2n+1}\text{OH} + 2_{n-1}\text{H}_2\text{O}$ and for carbon monoxide $\text{CO}_2 + \text{H}_2 \rightarrow \text{CO} + \text{H}_2\text{O}$.

The thermodynamic restriction limits the kinetics and requires a catalyst in order to reach the necessary reaction kinetics. The catalyst is characterized by two parameters: the preexponential factor k_0 and the activation energy E_A . Both have been determined for Co, Ni, Fe and Ru on Al₂O₃ in the reaction regime, where the reaction itself is limiting the rate, *i.e.* in the very

beginning of the conversion curve, when a sufficient amount is converted in order to perform an accurate measurement (Fig. 3, Table 1).^[15]

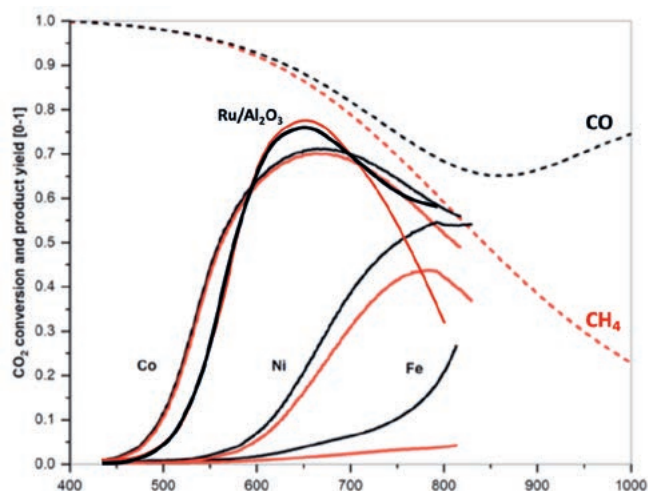


Fig. 3. Conversion yield of the reaction $\text{CO}_2 + 4\text{H}_2 \rightarrow \text{CH}_4 + 2\text{H}_2\text{O}$ and $\text{CO}_2 + \text{H}_2 \rightarrow \text{CO} + \text{H}_2\text{O}$ for Co, Ni, Fe and Ru/Al₂O₃. The thermodynamic limit is indicated with a dotted line. Reproduced with permission from ref [15], *J. Catal.* **2018**, 366, 139. Copyright 2018 American Chemical Society.

Ni and Ru as catalysts for the reduction of CO₂ to methane show the same activation energy, however, the Ru is approximately 50 times ($k_0 \cdot s_v$) more active than Ni. However, the specific surface area of Ni and Ru are 0.069 m²·g⁻¹ and 68 m²·g⁻¹, respectively, *i.e.* the Ru has 1000 times larger specific surface area than Ni. Finally, the Ni is per surface area (active sites) approximately 2.5 times more active than Ru.

2.2 Mechanism on the Supported Nanosized Catalysts

The mechanism of the CO₂ reduction on nanosized Ru supported on Al₂O₃ is shown in detail in Fig. 4.^[16,17] The first reaction step is the CO₂ adsorption as HCO₃* on Al₂O₃. Surface hydroxyl groups represent the acceptor sites for CO₂ according to $\text{CO}_2 + \text{OH}^* \rightarrow \text{HCO}_3^*$ at the interface of Ru and Al₂O₃. The second step is HCO₃* dissociating into CO* which binds on the Ru site. The dissociation temperature is high (400 K) under H₂-depletion conditions but takes place at room temperature in H₂-rich environments. The third step is CO* hydrogenation to CH₄ starting at 373 K, through a transition state, without detectable intermediates. If in H₂-rich conditions at the beginning, HCOO* at the interface also forms as the first step of CO₂ activation, then joins the CO* formation and hydrogenation steps.

The oxide support plays an important role in the CO₂ hydrogenation reaction on Ru/Al₂O₃. A catalyst composed of a metal

Table 1. The catalyst with the preexponential factor k_0 and the activation energy E_A , determined in the reaction limited region for the space velocity s_v (gas flow / reactor volume). The amount of catalyst in the microreactor $m(\text{catalyst})$ and the specific surface area of the catalyst A.

Catalyst	$m(\text{Catalyst})$ [g]	k_0 [s ⁻¹]	E_A [kJ·mol ⁻¹]	s_v [h ⁻¹]	A [m ² ·g ⁻¹]
Co	1	$(4.2 \pm 0.6) \cdot 10^5$	77 ± 3	965	1.1
Ni	1	$(1.0 \pm 0.2) \cdot 10^5$	74 ± 1	956	0.069
Fe	1	$(2.7 \pm 1) \cdot 10^2$	50 ± 1	1166	0.054
0.5 wt% Ru/Al ₂ O ₃	0.19	$(1.5 \pm 1.5) \cdot 10^6$	73 ± 2	5305	68

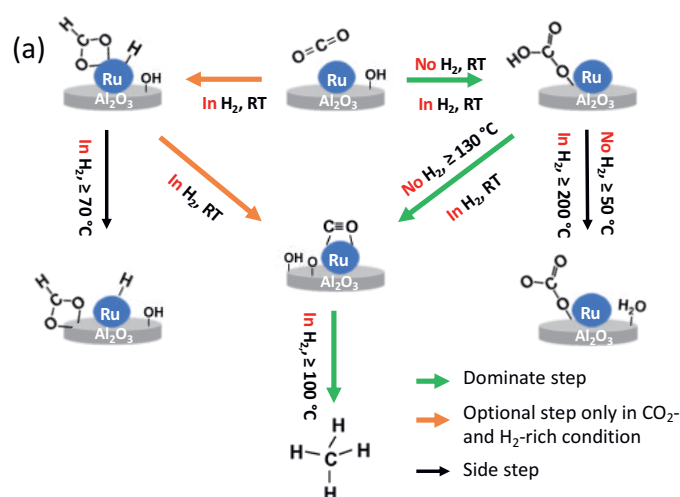


Fig. 4. CO₂ methanation pathway on Ru/Al₂O₃.

and its oxide like Co_x(CoO)_{1-x} with various ratio of metal/(metal + metal oxide) further specified the roles of the oxide and the metal.^[18] It shows that a higher ratio of CoO in the catalyst increases the activity for the CO₂ conversion. The same quantity of CO₂ conversion on the optimally composed Co and CoO, *i.e.* (Co_{0.2}(CoO)_{0.8}), is at much lower reaction temperature than on Ru/Al₂O₃ at the same reaction condition. For example, the 75% CO₂ conversion on Ru/Al₂O₃ occurred at 650 K, while the same conversion on Co_{0.2}(CoO)_{0.8} is reached at only 530 K. The origin of the distinct reactivity comes from the different capability of CO₂ chemisorption on the catalyst surface. The CO₂ chemisorption takes place on CoO, and is the rate-determining step of the overall hydrogenation reaction. The catalyst with high CoO concentration not only increased the amount of adsorbed CO₂, but also lowered the binding energy of CO₂ as compared to the catalyst with low CoO concentration. However, CoO did not act as catalytic center, the CO₂ reduction center is on metallic Co. Therefore, the catalyst with 80% CoO (20% metallic Co) reached the maximum activity among the catalysts with lower concentration of CoO. These results elucidate the optimal composition of metal and metal oxide for achieving the highest catalytic activity, and clarified the different active functions of the metal and metal oxide in the CO₂ hydrogenation reaction.

3. Electrochemical CO₂ Reduction

3.1 Catalysts and Products of Electrochemical CO₂ Reduction (eCO₂R)

To realize a closed energy cycle, H₂ for the hydrogenation of CO₂ must come from H₂O splitting driven by electrical energy from renewable sources such as solar and wind energy. Therefore, two reaction steps (H₂O → H₂ + O₂ and CO₂ + H₂ → products + H₂O) are required to store H₂ in the form of hydrocarbons. However, these two steps can be combined into a single electrochemical process, *i.e.* the direct electrochemical reduction of CO₂ (CO₂ + H₂O → C_xH_yO_z + O₂). In this process, the cathodic reaction is of the general form: xCO₂ + nH⁺ + ne⁻ → products + yH₂O, and the anodic reaction is the oxygen evolution reaction (2H₂O → O₂ + 4H⁺ + 4e⁻). As shown in Table 2, a variety of products can be electrochemically reduced from CO₂ including ones that cannot easily be prepared by a thermally driven process. More importantly, the electrochemical CO₂ reduction can run at room temperature and ambient pressure. Therefore, the direct electroreduction process is more suitable to decentralization than the thermal hydrogenation process, and the reaction can be quickly adjusted in order to match the overproduction of electricity from intermittent renewable sources.

As CO₂ is a thermodynamically rather stable molecule, and the CO₂ electroreduction reaction involves multiple proton-coupled electron transfer (PCET) processes, a more negative electrical potential than the theoretical potential is therefore required to achieve a sufficient production rate. Such overpotential could be detrimental, since it not only consumes additional electrical energy but also increases the evolution rate of H₂, which lowers both efficiency and selectivity. Therefore, to improve the activity and selectivity of the CO₂ electroreduction reaction, proper catalysts have to be used as the cathode material.

In the 1980s, Yoshio Hori and co-workers systematically investigated different metal electrodes for the electrochemical CO₂ reduction in aqueous electrolyte (*i.e.* 0.5 M KHCO₃).^[20] They successfully classified the metal catalysts into four groups according to their selectivity: Au, Ag and Zn are highly selective to CO (> 80% Faradaic efficiency); Sn, Pb, In and Bi produce primarily formate (HCOO⁻); Pt, Ni, Fe and Ti are highly selective for H₂ evolution instead of CO₂ reduction; and Cu is the only metal that can reduce CO₂ to hydrocarbons, aldehydes, and alcohols with substantial selectivity. The different selectivity of these four groups of metal catalysts can be explained by their different ability in binding the key reaction intermediates of eCO₂R and HER, including *H, *CO, *CHO, *COOH and *OCHO. Fig. 5 provides a simplified but effective classification of these metal catalysts according to their binding strength with *H and *CO. In this plot, Cu stands out from other metals with relatively weak binding energy with *H and strong with *CO, and thus can further reduce *CO and realize C–C coupling to produce hydrocarbons and oxygenates.

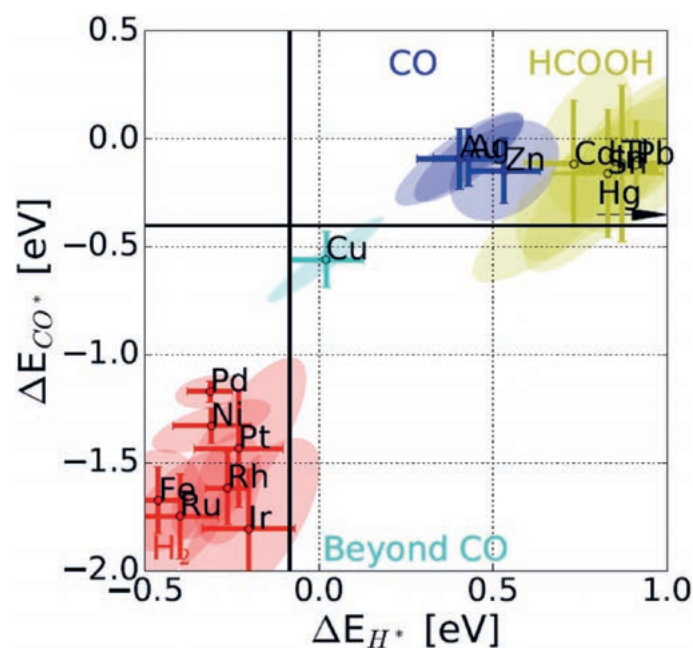


Fig. 5. Classification of metal catalysts for CO₂ electroreduction. Reproduced with permission from ref. [23], *ChemPhysChem* 2017, 18, 3266.

Following the pioneer work of Hori *et al.*, extensive efforts have been devoted on the development of advanced catalysts for eCO₂R. As the catalytic selectivity is governed by the adsorption of reaction intermediates, most of the studies have been focused on modulating the geometric and electronic structures of the catalysts, including alloying, doping, defect engineering, oxidation state regulation and facet control. In addition, other materials apart from metals are also found to be selective for eCO₂R. For exam-

Reaction	E ⁰ [V vs RHE]	Product
CO ₂ + 2H ⁺ + 2e ⁻ → HCOOH	-0.12	Formic acid
CO ₂ + 2H ⁺ + 2e ⁻ → CO	-0.10	Carbon monoxide
CO ₂ + 6H ⁺ + 6e ⁻ → CH ₃ OH + H ₂ O	0.03	Methanol
CO ₂ + 8H ⁺ + 8e ⁻ → CH ₄ + 2H ₂ O	0.17	Methane
2CO ₂ + 12H ⁺ + 12e ⁻ → C ₂ H ₅ OH + 3H ₂ O	0.09	Ethanol
2CO ₂ + 12H ⁺ + 12e ⁻ → C ₂ H ₄ + 4H ₂ O	0.08	Ethylene
2CO ₂ + 14H ⁺ + 14e ⁻ → C ₂ H ₆ + 4H ₂ O	0.14	Ethane
3CO ₂ + 18H ⁺ + 18e ⁻ → C ₃ H ₇ OH + 5H ₂ O	0.10	Propanol

Table 2. Electrochemical CO₂ reduction reactions with equilibrium potentials. The standard potentials are calculated via the Gibbs free energy of reaction using gas-phase thermochemistry data and, for aqueous products, Henry's Law data, from NIST.^[19]

ple, nitrogen-doped carbon materials, metal-single-atom catalysts (e.g. carbon supported Ni-single-atom catalysts) and molecular catalysts (e.g. cobalt phthalocyanine) are highly selective towards CO. Up to date, both CO and formate can be produced with a Faradaic efficiency of almost 100% at a current density higher than 200 mA cm⁻². For C₂H₄ generation, a Faradaic efficiency of 60% and a partial current density of 480 mA cm⁻² were achieved using a Cu electrode. In case of CH₃OH and C₂H₅OH, Faradaic efficiencies of 78/41% and partial current densities of 42/250 mA cm⁻² on Cu/Se and Ag/Cu catalysts have been achieved, respectively.^[21,22] Reducing CO₂ to products with longer carbon chains (e.g. more than three carbons) is still a big challenge due to the lack of efficient catalyst. Despite that the reported performance is still not satisfactory for practical applications, the fast development of the catalytic materials and the reaction mechanisms indicate that eCO₂R can be a potential strategy for storing renewable energy.

3.2 Studies of eCO₂R to CO, HCOOH and C₂₊ Products

CO₂ can be electrochemically reduced to various products and among them, the production of 2e⁻ products (CO and HCOOH) is economically more feasible for being implemented on a large scale. This is due to the fact that at the present state of development, CO and HCOOH can be produced with relatively high selectivity and low overpotential. Nevertheless, improvement on the catalytic performance, in terms of activity, selectivity and stability, is still required before any industrial applications. In order to enhance the CO₂ to CO performance, a recent work reported the preparation of the Cu nanowire supported In nanoparticle catalyst using a facile dip-coating method.^[24] The final material provided a high density of Cu–In interfaces and showed over 90% CO Faradaic efficiency during 60 h operation at -0.6V versus reversible hydrogen electrode (V vs. RHE). Combining the bulk

and surface characterization results and density functional theory (DFT) simulation, the origin of the high CO selectivity was suggested to be the presence of the Cu–In interface, which prefers the adsorption of the reaction key intermediate (*COOH). This demonstrates that engineering the bimetallic interactions can effectively improve the intrinsic activity and selectivity for eCO₂R. On the other hand, the catalytic performance can also be enhanced by increasing the number of active sites.^[25]

Since Cu catalysts can reduce CO₂ to as many as 16 products, the distinct reaction environment would strongly affect the reaction pathways. Self-supported Cu-based catalysts can be applied to study the influence of electrolyzer on the catalytic performance. The catalysts exhibit high selectivity (>40%) for converting CO₂ to C₂₊ products (e.g. C₂H₄ and ethanol), at >100 mA cm⁻² in flow reactor using 1 M KOH as electrolyte.^[26] When aiming for multicarbon products, it is important to assess the catalytic performance of the catalysts in flow reactors under industrial relevant conditions (Fig. 6).

4. Applications & Economy

4.1 Methane Reactor with Temperature Gradient

The Sabatier reaction was discovered by French chemists Paul Sabatier and Jean-Baptiste Senderens in 1897. The process produces methane and water from a reaction of hydrogen with carbon dioxide at high temperatures (optimally 200–400 °C) and at moderate pressures (5–30 bar) in the presence of a catalyst such as nickel or ruthenium on alumina (aluminum oxide). Despite the fact that CO₂ + 4H₂ → CH₄ + 2H₂O is a fairly simple chemical reaction, we still do not know what the mechanism and especially the transition states are. The reaction is exothermic and the change entropy is negative as with most hydrocarbon products. Because

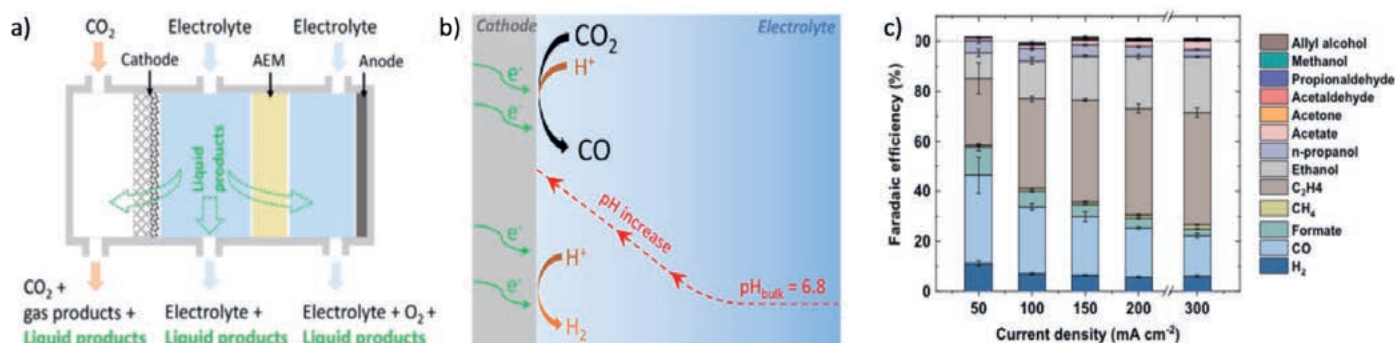


Fig. 6. a) Schematic illustration of liquid products crossover in flow reactor. b) Schematic illustration of local pH effect. Reproduced with permission from ACS Catal. 2019, 9, 3783-3791. c) Faradaic efficiency of the Cu catalyst with considering the products crossed in the other chambers. Reproduced with permission from J. Catal. 2020, 385, 140-145. © American Chemical Society 2020.

only CO is also stable under the reaction conditions and CH₄ does not require any CC coupling, the reaction is rather selective. However, a hot spot can develop at the entry of gas which limits the life of the catalyst and reduces the amount of product formed. Sabatier reactors have been developed and built for over 100 years with the objective of avoiding this hot spot and to create a homogeneous temperature distribution. Consequently, the yield of the reaction at 400 °C is limited to about 70% of CO₂ conversion. We have developed a new type of reactor where the catalyst bed is cooled with water tubes creating a high temperature gradient (Fig. 7). The reaction is fast in the hot regions beside the gradient, where the reaction ends along the thermodynamic limit resulting in a CO₂ conversion of 99.6% in a single stage reactor.^[27] This concept allows the construction of new highly efficient and small (high power) reactors and does not require any after treatment of the product gases except the condensation of the water.

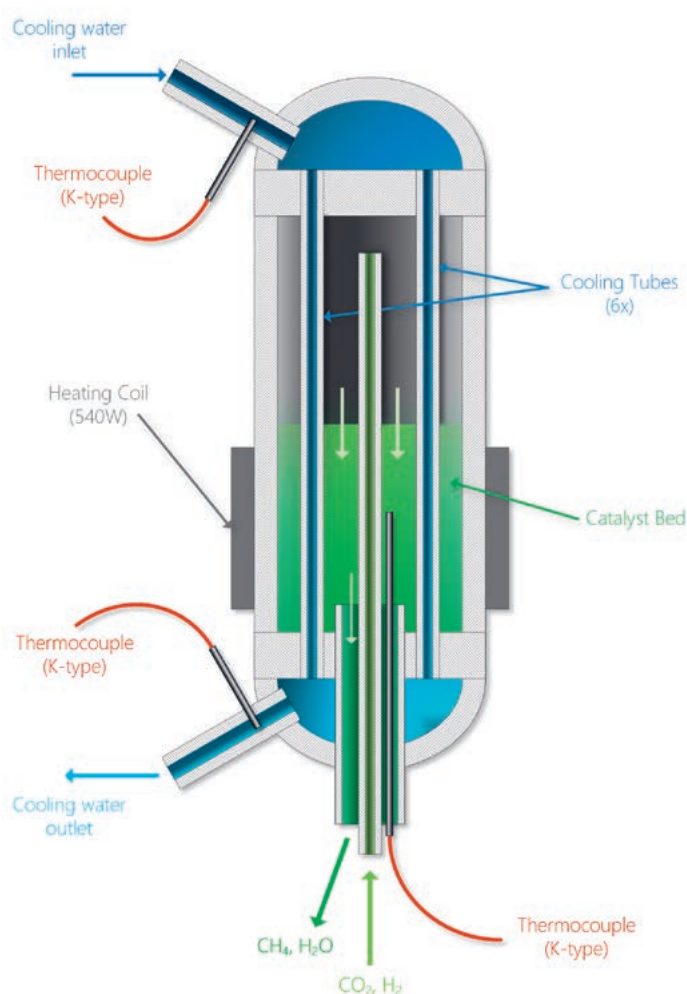


Fig. 7. Small 2 kW methane reactor cross-section, water cooling in blue, Reaction bed in green. Reproduced with permission from ref. [26], *J. Mater. Chem. A* 2019, 7, 26285.

4.2 Upscaled Methane Reactor with the Use of Heat

From a 2 kW reactor in the EPFL laboratory, a 20 kW reactor was developed in collaboration with Gaznat for the gas metering and regulation station in Sion (Switzerland). Since the upscaling retained all the benefits for the reaction and at the same time recovered the waste heat from the chemical reaction, a very high product yield combined with near 100% energy efficiency was achieved.^[28] The upscaled reactor consists, in addition to the tubular cooling system, three reaction zones with decreasing average temperature and increasing reaction time.

4.3 Optimized Industrial Methane Reactor

Building on this very successful development, a new 200 kW reactor is currently under planning by EPFL, Gaznat and GRZ Technologies. The reactor can be used not only to convert renewable hydrogen and CO₂ from the atmosphere or flue gas to CO₂ neutral synthetic methane, but also offers the possibility of converting biogas, which contains up to 50% of CO₂, to methane without the need to separate CO₂ and bio-methane before moving forward. This almost doubles the production of methane from biogas without requiring an expensive separation process.

4.4 Cost of Synthetic Hydrocarbons

The minimum energy necessary, the thermodynamic limit, for CO₂ capture depends on the CO₂ concentration and at 10% (in typical flue gas) and 400 ppm (in air) amounts to 36 Wh/kg and 120 Wh/kg,^[29] respectively, the latter being less than 5% of the heating value of the hydrocarbon produced from CO₂ and hydrogen. The cost of CO₂ capture from air is estimated to be <0.5 CHF/kg CO₂, and with optimization^[30] of the energy source and the process, the cost may be reduced to <0.22 CHF/kg CO₂. An example of an installed system for the capture of CO₂ from air produces 2500 kg CO₂ per day and has an investment of 3.6 million CHF (1500 CHF/(kg CO₂/day)). The estimated energy requirement for CO₂ absorption is 300 Wh_{el}/kg CO₂ for air ventilation and 2 kWh/kg CO₂ for desorption of CO₂.^[31] Whereas the ventilation energy is electric energy, the desorption heat can be provided by waste heat sources (>100 °C), if they are available (Fig. 8).

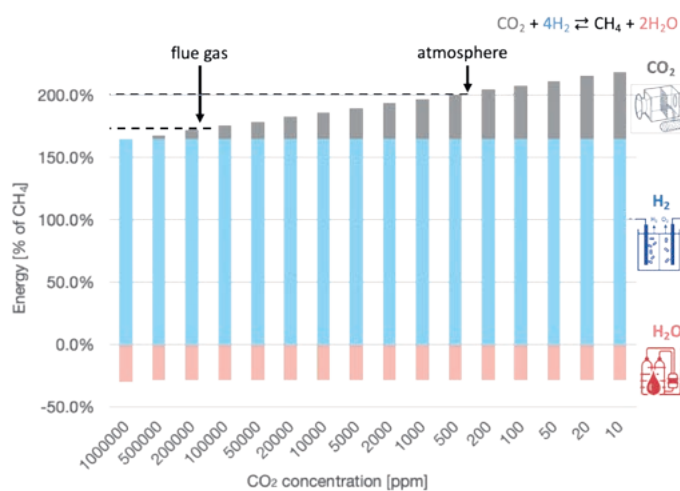


Fig. 8. Energy demand relative to the energy in the synthesized hydrocarbon in %. Currently available systems for CO₂ capture require 4 to 5 times the energy shown in the figure and as a consequence the energy demand for the CO₂ capture exceeds the energy demand for electrolysis.

The cost of synthetic fuel is estimated from the energy cost and the capital expenditure with the life time, the transferred energy. Assuming photovoltaics cost to be 1200 CHF/kW_p (completely installed panels) with a lifetime of 20 years results in an electricity cost of 0.075 CHF/kWh. The current synthesis of alkanes from CO₂, e.g. octane (8CO₂ + 25H₂ → C₈H₁₈ + 16H₂O), converts 7 kg CO₂ with 1 kg H₂ to 2.3 kg octane and conserves 57% of the energy in hydrogen. The exothermic reaction provides 2.3 kWh of heat at >200 °C per 1 kg CO₂. The synthesis plant Pearl GTL facility in Qatar^[32] produces 140000 barrels of oil per day (10 GW) and has a cost of 18 BCHF (1800 CHF/kW). This unique example shows that on a large scale, the synthesis of hydrocarbons (Fischer-Tropsch synthesis) requires an investment of close to 2300 CHF/kW. The cost of hydrogen production from renewable energy is estimated to be approximately 10 CHF/kg H₂ and

the synthetic hydrocarbons costs approximately 4.5 CHF/kg or 0.3 CHF/kWh. Approximately 60% are capital and operational costs and 40% are energy costs.

5. Conclusions

The seasonal storage of renewables is the biggest challenge in replacing fossil fuels with renewables. Renewable energy can be converted by electrolysis with a yield >80% with the technology available today followed by the synthesis of methane with CO₂ air capture, using the heat of the methane reaction. This provides synthetic methane with a high yield and high energy efficiency that is stored underground in very large quantities >1 TWh per storage unit. This technology will allow the seasonal storage of renewable energy on a national relevant scale without affecting the environment and without the need of mountains for the installation of large hydroelectric power stations.

The prospective application beside renewable energy storage of the heterogeneously catalyzed gas phase reduction of CO₂ is the upgrade of biogas with hydrogen produced by renewable energy. This allows to double the quantity of green methane produced and to substitute the amine wash to remove the residual CO₂ in biogas.

The electrochemical CO₂ reduction has the potential to be applied on a small scale for individual homes as well, where excess PV power during the summer time could be stored in produced ethanol. The other important application of the electrochemical CO₂ reduction is to utilize the process in seawater that contains CO₂. This is especially interesting for marine applications, also in regions where the solar intensity is high.

Acknowledgement

The financial support by SCCER Heat and Energy Storage (innosuisse) is greatly acknowledged.

Received: January 5, 2021

- [1] K. S. Lackner, S. Brennan, J. M. Matter, a-H. A. Park, A. Wright, B. van der Zwaan, *Proc. Natl. Acad. Sci. USA* **2012**, *109*, 13156, <https://doi.org/10.1073/pnas.1108765109>
- [2] A. Züttel, P. Mauron, S. Kato, E. Callini, M. Holzer, J. Huang, *CHIMIA* **2015**, *69*, 264, <https://doi.org/10.2533/chimia.2015.264>
- [3] B. C. Gates, *Angew. Chem.* **1993**, *32*, 228, <https://doi.org/10.1002/anie.199302281>
- [4] C. K. Rofer-DePoorter, *Chem. Rev.* **1981**, *81*, 447, <https://doi.org/10.1021/cr00045a002>
- [5] http://www.fischer-tropsch.org/DOE/DOE_reports/510/510-34929/510-34929.pdf, P. L. Spath, D.C. Dayton, 'Preliminary Screening — Technical and Economic Assessment of Synthesis Gas to Fuels and Chemicals with Emphasis on the Potential for Biomass-Derived Syngas', NREL/TP510-34929, **2003**, pp. 95.
- [6] B. H. Davis, *Fuel Proc. Technol.* **2001**, *71*, 157, [https://doi.org/10.1016/S0378-3820\(01\)00144-8](https://doi.org/10.1016/S0378-3820(01)00144-8)
- [7] http://www.exxonmobil.com/Apps/RefiningTechnologies/files/sellsheet_09_mtg_brochure.pdf
- [8] http://en.wikipedia.org/wiki/Fischer-Tropsch_process.
- [9] P. Stelmachowski, S. Sirotnin, P. Bazin, F. Maugé, A. Travert, *Phys. Chem. Chem. Phys.* **2013**, *15*, 9335, <https://doi.org/10.1039/C3CP51146D>
- [10] J. H. Montoya, A. A. Peterson, J. K. Nørskov, *ChemCatChem* **2013**, *5*, 737, <https://doi.org/10.1002/cctc.201200564>
- [11] J. Wei, Q. Ge, R. Yao, Z. Wen, C. Fang, L. Guo, H. Xu, J. Sun, *Nat. Commun.* **2017**, *8*, 15174, <https://doi.org/10.1038/ncomms15174>
- [12] P. Gao, S. Li, X. Bu, S. Dang, Z. Liu, H. Wang, L. Zhong, M. Qiu, C. Yang, J. Cai, W. Wei, Y. Sun, *Nat. Chem.* **2017**, *9*, 1019, <https://doi.org/10.1038/nchem.2794>
- [13] C. Xie, C. Chen, Y. Yu, J. Su, Y. Li, G. A. Somorjai, P. Yang, *Nano Lett.* **2017**, *17*, 3798, <https://doi.org/10.1021/acs.nanolett.7b01139>
- [14] N. Ladygina, E. G. Dedyukhina, M. B. Vainshtein, *Proc. Biochem.* **2006**, *41*, 1001, <https://doi.org/10.1016/j.procbio.2005.12.007>
- [15] R. Mutschler, E. Moiola, W. Luo, N. Gallandat, A. Züttel, *J. Catal.* **2018**, *366*, 139, <https://doi.org/10.1016/j.jcat.2018.08.002>
- [16] K. Zhao, L. Wang, M. Calizzi, E. Moiola, A. Züttel, *J. Phys. Chem. C* **2018**, *122*, 20888, <https://doi.org/10.1021/acs.jpcc.8b00061>
- [17] K. Zhao, L. Wang, E. Moiola, M. Calizzi, A. Züttel, *J. Phys. Chem. C* **2019**, *123*, 8785, <https://doi.org/10.1021/acs.jpcc.8b11105>
- [18] K. Zhao, M. Calizzi, E. Moiola, M. Li, A. Borsay, L. Lombardo, R. Mutschler, W. Luo, A. Züttel, *J. Energy Chem.* **2021**, *53*, 241, <https://doi.org/10.1016/j.jechem.2020.05.025>
- [19] S. Nitopi, E. Bertheussen, S. B. Scott, X. Liu, A. K. Engstfeld, S. Horch, B. Seger, I. E. L. Stephens, K. Chan, C. Hahn, J. K. Nørskov, T. F. Jaramillo, I. Chorkendorff, *Chem. Rev.* **2019**, *119*, 7610, <https://doi.org/10.1021/acs.chemrev.8b00705>
- [20] Y. Hori, 'Electrochemical CO₂ Reduction on Metal Electrodes', in 'Modern Aspects of Electrochemistry', **2008**, No. 42, Springer, New York.
- [21] D. Yang, Q. Zhu, C. Chen, H. Liu, Z. Liu, Z. Zhao, X. Zhang, S. Liu, B. Han, *Nat. Commun.* **2019**, *10*, 677, <https://doi.org/10.1038/s41467-019-08653-9>
- [22] Y. C. Li, Z. Wang, T. Yuan, D.-H. Nam, M. Luo, J. Wicks, B. Chen, J. Li, F. Li, F. P. García de Arquer, Y. Wang, C.-T. Dinh, O. Voznyy, D. Sinton, E. H. Sargent, *J. Am. Chem. Soc.* **2019**, *141*, 8584, <https://doi.org/10.1021/jacs.9b02945>
- [23] A. Bagger, W. Ju, A. S. Varela, P. Strasser, J. Rossmeis, *ChemPhysChem* **2017**, *18*, 1, <https://doi.org/10.1002/cphc.201700736>
- [24] W. Luo, W. Xie, R. Mutschler, E. Oveisi, G. L. De Gregorio, R. Buonsanti, A. Züttel, *ACS Catal.* **2018**, *8*, 6571, <https://doi.org/10.1021/acscatal.7b04457>
- [25] W. Luo, W. Xie, M. Li, J. Zhang, A. Züttel, *J. Mater. Chem. A* **2019**, *7*, 4505, <https://doi.org/10.1039/C8TA11645H>
- [26] J. Zhang, W. Luo, A. Züttel, *J. Mater. Chem. A* **2019**, *7*, 26285, <https://doi.org/10.1039/C9TA06736A>
- [27] N. Gallandat, R. Mutschler, V. Vernay, H. Yang, A. Züttel, *Sus. Energy Fuels* **2018**, *2*, 1101, <https://doi.org/10.1039/C8SE00073E>
- [28] E. Moiola, N. Gallandat, A. Züttel, *Chem. Eng. J.* **2019**, *375*, 121954, <https://doi.org/10.1016/j.cej.2019.121954>
- [29] K. S. Lackner, S. Brennan, J. M. Matter, A.-H. A. Park, A. Wright, B. van der Zwaan, *Proc. Natl. Acad. USA* **2012**, *109*, 13156, <https://doi.org/10.1073/pnas.1108765109>
- [30] M. Fasihi, O. Efimova, C. Breyer, *J. Cleaner Prod.* **2019**, *224*, 957, <https://doi.org/10.1016/j.jclepro.2019.03.086>
- [31] B. Vogel, 'CO₂ – der Rohstoff, der aus der Luft kommt', im Auftrag des Bundesamts für Energie (BFE) Stand: Mai **2017**; given values are estimations from Climeworks for the future, the energy consumption of current systems are 4–8 times higher.
- [32] https://en.wikipedia.org/wiki/Pearl_GTL

License and Terms



This is an Open Access article under the terms of the Creative Commons Attribution License CC BY 4.0. The material may not be used for commercial purposes.

The license is subject to the CHIMIA terms and conditions: (<http://chimia.ch/component/sppagebuilder/?view=page&id=12>).

The definitive version of this article is the electronic one that can be found at <https://doi.org/10.2533/chimia.2021.156>